https://doi.org/10.30799/jnst.359.25100301 J. Nanosci. Tech. - Volume 10 Issue 3 (2025) 1006–1011

Share Your Innovations through JACS Directory

Journal of Nanoscience and Technology

Visit Journal at https://www.jacsdirectory.com/jnst

ISSN: 2455-0191

Solution-Grown Transparent ZnS Ultra-Thin Nanostructured Films for Photocatalytic Degradation of Methyl Red

Deepti Gupta[1], Trapti Gupta[1,*], Ramphal Sharma[2], Gunjan Soni[1]

[1]*Department of Chemistry, IIS(Deemed to be) University, Jaipur – 302020, Rajasthan, India.*
[2]*Department of Physics, IIS(Deemed to be) University, Jaipur – 302020, Rajasthan, India.*

ARTICLEDETAILS

Article history:
Received 19 May 2025
Accepted 04 June 2025
Available online 15 June 2025

Keywords:
Zinc Sulfide (ZnS) Thin Films
Dye Degradation
Photocatalysts
Water Purification

ABSTRACT

Rapid industrialization and urbanization have intensified global water contamination, necessitating sustainable and cost-effective treatment solutions. Semiconductor-based photocatalysis, which utilizes solar energy for advanced oxidation processes, offers a promising green technology. This study focuses on the synthesis of transparent zinc sulfide (ZnS) ultra-thin nanostructured films via chemical bath deposition (CBD) and their application in the photocatalytic degradation of methyl red dye, a common organic pollutant. The structural, morphological, and optical properties of ZnS films were analyzed using XRD, FESEM, and EDAX. XRD confirmed the cubic zinc blende structure with high crystallinity, a 19.11 nm average crystallite size, low dislocation density (0.0036 nm^{-2}), and minimal microstrain (0.0018), enhancing photocatalytic performance. FESEM revealed a uniform nanorod morphology with increased surface area and efficient charge carrier dynamics, while EDAX verified the films' elemental purity. Using ultraviolet radiation from sunlight, ZnS films achieved 97% degradation of methyl red within 60 minutes. This exceptional photocatalytic performance is attributed to their high crystallinity, optimized nanostructure, and photothermal properties, which enhanced photon absorption, reduced electron-hole recombination, and facilitated reactive oxygen species generation. This research highlights the potential of transparent ZnS ultra-thin nanostructured films as an efficient and sustainable photocatalyst for advanced water treatment applications, leveraging sunlight for eco-friendly and energy-efficient dye degradation. These findings contribute significantly to global efforts in environmental remediation and sustainable water purification.

1. Introduction

The rapid urbanization and industrial expansion in recent decades have significantly strained global water resources, resulting in severe contamination challenges. Effective water purification is a critical environmental priority, yet conventional wastewater treatment techniques - such as sedimentation, chlorination, membrane filtration, and reverse osmosis - exhibit inherent limitations, including high energy demands, excessive sludge production, secondary pollutant generation, and substantial operational costs. These drawbacks necessitate the development of sustainable, efficient, and eco-friendly alternatives for water treatment [1]. Semiconductor-based photocatalysis has emerged as a promising green technology for addressing water pollution by harnessing solar energy to drive advanced oxidation processes (AOPs) [2]. Through photon absorption and the generation of electron-hole pairs, semiconductor photocatalysts degrade organic pollutants into harmless byproducts, such as water and carbon dioxide. Among various semiconductor materials, zinc sulfide (ZnS), an n-type semiconductor, has gained significant attention due to its desirable physical and chemical properties, including a wide bandgap (3.68 eV), high electron mobility, thermal stability, and economic viability [2,3].

Despite its potential, the practical application of ZnS is limited by rapid electron-hole recombination, insufficient utilization of the solar spectrum, and photo-corrosion under prolonged light exposure. To address these limitations, researchers have focused on nanostructured ZnS materials, particularly ultra-thin films, which offer enhanced photocatalytic performance through increased surface-to-volume ratios, improved charge carrier dynamics, and tunable optical properties [4].

ZnS exists in two primary crystalline phases: sphalerite (cubic) and wurtzite (hexagonal). While the sphalerite phase is stable at room temperature, it transitions to the wurtzite phase at higher temperatures (~1020 °C) [5]. Both phases primarily absorb UV light due to their wide bandgap, which limits their activity to wavelengths below 340 nm. However, since UV light constitutes only ~4% of sunlight, strategies such as morphology control and bandgap engineering are crucial to extending ZnS activity into the visible light spectrum.

This study investigates transparent ZnS ultra-thin nanostructured films synthesized via chemical bath deposition (CBD) at varying deposition times [6]. Structural, morphological [7], and optical characterizations were performed to optimize the photocatalytic properties of the films [8]. efficacy in degrading methyl red dye, a common organic pollutant [9], was evaluated to demonstrate their potential for advanced water treatment applications [8-10]. These findings highlight the role of ZnS nanostructured thin films in advancing wastewater purification technologies and addressing global environmental challenges [1,3,11].

2. Materials and Methods

2.1 Materials

All chemicals used in this study were of analytical grade and used without further purification. Zinc chloride dihydrate, thiourea, TEA, ammonia, and methyl red were procured from Sigma-Aldrich. Deionized water was utilized as the solvent throughout the experimental process.

2.2 Synthesis of ZnS Nanostructured Films

The nanostructured ZnS films were synthesized using the CBD technique, a simple and cost-effective method to fabricate thin films with controlled morphology and properties [12].

2.2.1 Preparation of Solutions

Solution A: Zinc chloride dihydrate (0.02 M) was dissolved in deionized water, and ammonia (NH_3) was added to form a zinc-ammonia complex. The mixture was stirred continuously at room temperature for 15 minutes to ensure complete dissolution and homogeneity.

*Corresponding Author:trapti.gupta@iisuniv.ac.in(Trapti Gupta)

https://doi.org/10.30799/jnst.359.25100301

Cite this Article as: Deepti Gupta, Trapti Gupta, Ramphal Sharma, Gunjan Soni, Solution-grown transparent ZnS ultra-thin nanostructured films for photocatalytic degradation of methyl red, J. Nanosci. Tech. 10(3) (2025) 1006–1011.

Solution B: Thiourea (0.02 M) was dissolved in deionized water with constant stirring for 15 minutes at room temperature to obtain a clear and homogeneous solution [13,14].

After preparing the individual solutions, Solution A and Solution B were mixed together. To this combined solution, three drops of triethanolamine (TEA) were added as a complexing agent to regulate the controlled release of Zn^{2+} ions, preventing rapid precipitation. The pH of the resulting solution was adjusted to 11 using ammonia, creating an alkaline environment essential for the deposition process. The mixture was subsequently heated to 80 °C.

2.2.2 Deposition Process

ZnS thin films were deposited at varying deposition times to investigate their growth kinetics and the effect on film properties. Glass substrates were pre-cleaned with acetone and deionized water before immersion in the chemical bath. The deposition process was carried out at a constant temperature of 80 °C for deposition times of 1, 2, 3, and 4 hours. The variation in deposition time allowed for a comprehensive analysis of changes in film thickness, morphology, and photocatalytic properties.

2.3 Mechanism for the Formation of ZnS Thin Film

The formation of ZnS thin films using zinc chloride dihydrated ($ZnCl_2.2H_2O$), thiourea, ammonia, and TEA involves a CBD process. (i) Dissolution and Complex Formation $ZnCl_2$ dissolves in water, dissociating into Zn^{2+} ions:

$$ZnCl_2 \rightarrow Zn^{2+} + 2Cl^-$$

Complexation with TEA: TEA acts as a complexing agent by forming a soluble zinc-TEA complex, represented as:

$$Zn^{2+} + TEA \rightarrow [Zn(TEA)]^{2+}$$

This complex controls the release of Zn^{2+} ions in the solution, preventing their premature precipitation. The gradual release of Zn^{2+} ions from the TEA complex ensures uniform film growth, contributing to the controlled deposition process,

(ii) *Sulfur Source* (Thiourea): Thiourea acts as the sulfur source and undergoes hydrolysis in an alkaline medium (provided by ammonia). The hydrolysis releases S^{2-} ions:

$$(NH_2)_2C{=}S + OH^- \rightarrow H_2O + NH_3 + H_2S$$
$$H_2S \rightarrow H^+ + HS^- \rightarrow H^+ + S^{2-}$$

(iii) *Role of Ammonia*: Ammonia plays a crucial role in maintaining the pH of the solution at around 11, which is essential for proper complex formation and the controlled release of ions. Additionally, it prevents the immediate precipitation of $Zn(OH)_2$ or other intermediates by forming soluble zinc-ammonia complexes, thereby ensuring a stable environment for uniform thin film deposition[15].

$$Zn^{2+} + 4NH_3 \rightarrow [Zn(NH_3)_4]^{2+}$$

(iv) *Formation of ZnS Thin Film*: When the solution is heated to around 60°C, the thermal energy drives the decomposition of complexes and releases Zn^{2+} and S^{2-} ions. These ions then react to form ZnS on the substrate:

The Zn complexes act as sources of Zn^{2+} ions. In the alkaline solution, these complexes dissociate partially to release Zn^{2+}[5]:

$$[Zn(TEA)] \leftrightarrow Zn^{2+} + TEA$$
$$[Zn(NH_3)_4]^{2+} \leftrightarrow Zn^{2+} + 4NH_3$$

The Zn-TEA complex is more stable than the Zn-NH_3 complex, releasing Zn^{2+} ions at a slower and more controlled rate. This gradual release ensures uniform deposition and smooth film growth. In contrast, the Zn-NH_3 complex dissociates more readily, providing an initial burst of Zn^{2+} ions that facilitates nucleation.

$$Zn^{2+} + S^{2-} \rightarrow ZnS \text{ (thin film)}$$

As the ZnS nuclei form in the solution, they deposit onto the pre-cleaned glass substrate through a combination of heterogeneous nucleation and ion-by-ion growth [15, 16]. In heterogeneous nucleation, ZnS forms directly on the substrate surface, providing a foundation for further growth. Simultaneously, in the ion-by-ion growth process, Zn^{2+} and S^{2-} ions diffuse to the growing ZnS surface, where they combine to extend the film layer, resulting in the gradual buildup of the ZnS thin film.

2.4 Physical Measurements

The FTIR spectrum of the synthesized ZnS nanoparticles was recorded using KBr pellets on a Bruker Optics FTIR spectrophotometer (Germany) to identify functional groups and confirm chemical bonding. The powder XRD pattern was obtained on a Panalytical X'pert Pro MPD diffractometer equipped with Ni-filtered Cu Kα radiation (λ = 1.54060 Å) operating at 45 kV and 40 mA to determine the crystal structure and phase purity of the samples. UV-Vis absorption spectra were recorded at room temperature using a SHIMADZU UV-1800 UV-Vis spectrophotometer to analyze the optical properties and calculate the bandgap energy. Surface morphology and elemental composition were examined using field emission scanning electron microscopy (FESEM) and energy-dispersive X-ray analysis (EDAX) on a Nova Nano SEM 450.

2.5 Photocatalytic Activity

Methyl red degradation under sunlight is inherently slow due to insufficient energy in sunlight to directly excite dye molecules. However, the use of photocatalysts like ZnS semiconductors significantly enhances the degradation process [4,11]. ZnS absorbs the UV rays present in sunlight, initiating photocatalytic activity through the generation of electron-hole pairs. These pairs react with water and oxygen, leading to the formation of reactive oxygen species (ROS), such as hydroxyl radicals (•OH), superoxide ions ($O_2•^-$), and hydrogen peroxide (H_2O_2). ROS are highly reactive and play a crucial role in breaking down organic pollutants like methyl red. The activity of ZnS thin films was investigated by immersing them in aqueous methyl red solutions for 10-60 minutes, followed by drying and analysis using UV-Vis spectroscopy [10].

ZnS nanoparticles have been widely studied for their photocatalytic potential in degrading organic dyes. Hydroxyl radicals, in particular, effectively target the azo (-N=N-) group of methyl red, initiating molecular degradation. This process leads to the breakdown of bonds within the dye, ultimately producing environmentally benign intermediates like carbon dioxide and water. The photocatalytic performance of ZnS is closely linked to its structural and optical properties, which govern the efficiency of ROS generation and their interaction with pollutants [3,17].

2.6 Removal Efficiency of Degradation

The photocatalytic activity of ZnS nanoparticles was evaluated by monitoring the degradation efficiency of methyl red dye over time. The degradation efficiency (%) was calculated using the formula:

$$\text{Degradation Efficiency} = \frac{C_0 - C_t}{C_0} \times 100 \qquad (1)$$

where C_0 and C_t are the initial and time-dependent concentrations of methyl red dye, respectively.

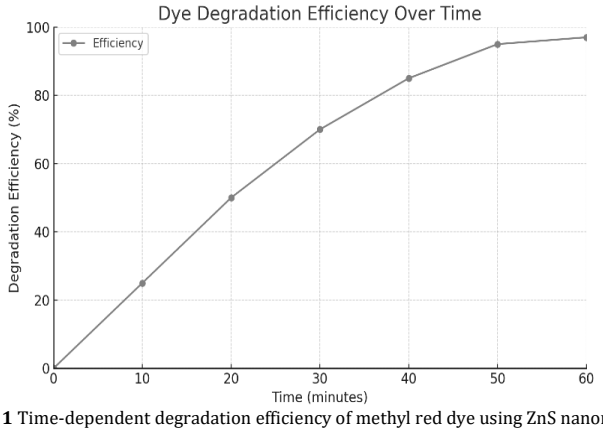

Fig. 1 Time-dependent degradation efficiency of methyl red dye using ZnS nanorods as photocatalysts under UV rays from sunlight

The graph (Fig. 1) illustrates the degradation efficiency over a time interval of 0 to 60 minutes, achieving 97% degradation efficiency by the end of the reaction. The degradation process involves the absorption of UV rays from sunlight by ZnS nanoparticles, which initiates photocatalytic activity through the generation of electron-hole pairs. These charge carriers react with water and oxygen to produce reactive species such as hydroxyl radicals (•OH) and superoxide radicals ($•O_2^-$), which actively degrade dye molecules. The photocatalytic performance of ZnS nanoparticles under UV radiation from sunlight underscores their potential for the effective removal of organic pollutants from wastewater, making them a promising solution for environmental remediation applications [18].

https://doi.org/10.30799/jnst.359.25100301

Cite this Article as: Deepti Gupta, Trapti Gupta, Ramphal Sharma, Gunjan Soni, Solution-grown transparent ZnS ultra-thin nanostructured films for photocatalytic degradation of methyl red, J. Nanosci. Tech. 10(3) (2025) 1006–1011.

3. Results and Discussion

3.1 NP's Production: Photothermal Effect

The photothermal effect involves converting light energy into heat, which enhances ZnS thin film performance in photocatalysis. UV radiation from sunlight generates electron-hole pairs and localized surface heating. This heat improves charge carrier mobility, reduces recombination rates, and enhances ROS generation. During ZnS nanoparticle synthesis, the photothermal effect promotes better crystallization and controlled morphology. Elevated surface temperatures during deposition improve film crystallinity and optical properties, such as the bandgap. These effects are more pronounced with longer deposition times in the CBD process, yielding ZnS thin films with superior photocatalytic efficiency.

Additionally, the photothermal effect aids in optimizing nanoparticle size and distribution, further enhancing catalytic activity. This mechanism is not limited to ZnS but applies to other semiconductors, emphasizing the importance of photothermal strategies in designing efficient photocatalysts for environmental remediation.

3.2 Characterizations

3.2.1 XRD Analysis

The X-ray diffraction (XRD) analysis was carried out to investigate the crystalline structure and phase purity of the synthesized ZnS nanostructured thin films. The structural characterization was performed using XRD in the 2θ range of 10°-80°. The XRD pattern of the transparent nanostructured ZnS ultrathin film, shown in Fig. 2, reveals sharp and intense peaks, which indicate high crystallinity. This high crystallinity is essential as it directly influences the material's electronic properties, which are crucial for its photocatalytic performance. The XRD peaks observed at 2θ values of 28.38°, 34.27°, 47.11°, 56.51°, 59.62°, and 63.17° correspond to the Miller indices (hkl) of (111), (200), (220), (311), (222), and (400), respectively. These peaks are indicative of the cubic zinc blende structure of ZnS [19,20]. The peak positions are in good agreement with the standard diffraction pattern for cubic ZnS, as referenced in JCPDS Card No. 005-0566 [21,22].

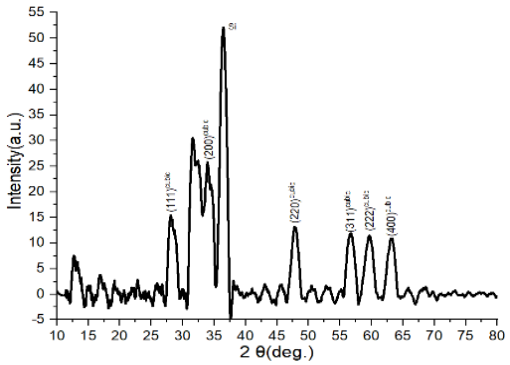

Fig. 2 X - ray diffraction patterns of nanostructured ZnS ultra thin film

In addition to the peaks associated with the ZnS crystal planes, additional peaks are also present in the XRD pattern. These extra peaks are likely attributed to the substrate material used for film deposition, such as glass, which contains silicon and other components that may contribute to the overall diffraction pattern.

Furthermore, the average crystallite size of the nanostructured ZnS can be estimated using the Scherer's formula shown in Eq.(2) [23],

$$D(hkl) = \frac{k\lambda}{\beta Cos\theta} \quad (2)$$

where D is the crystallite size, k is the shape factor (typically around 0.9), λ is the X-ray wavelength (1.5406 Å for Cu Kα radiation), β is the full width at half maximum (FWHM) of the peak in radians, and θ is the Bragg angle. The synthesized ZnS nanostructures were found to have an average crystallite size of approximately 19.11 nm, as calculated using the Scherrer formula, which aligns well with the nanorod morphology observed in other characterization techniques. XRD analysis confirms that the ZnS nanostructures exhibit a highly crystalline cubic structure with excellent phase purity, further highlighting their suitability for advanced photocatalytic applications.

$$\partial = \frac{1}{D^2} \quad (3)$$

$$\varepsilon = \frac{\beta \cos\theta}{4} \quad (4)$$

The low dislocation density (0.0036 nm^{-2}) and microstrain (0.0018), calculated using Eqs.(3) and (4) and presented in Table 1, reflect the exceptional crystalline quality of the material, characterized by minimal lattice defects [16]. This structural refinement significantly enhances the optical and electronic properties of ZnS. The low dislocation density reduces defect-related trapping sites, minimizing electron-hole recombination and enhancing charge carrier mobility and separation. Reduced microstrain ensures fewer lattice distortions, leading to improved crystallinity, enhanced photon absorption, and minimized light scattering [24]. These structural advantages also improve surface reactivity by facilitating efficient adsorption of reactants and stronger interactions with target molecules. Furthermore, the enhanced structural stability ensures the material's durability during repeated photocatalytic cycles. Collectively, these attributes make ZnS nanostructures highly efficient for photocatalytic applications. In particular, they exhibit superior performance in the degradation of methyl red dye, a common water pollutant. The high crystalline quality and low defect density enhance the separation and lifespan of photogenerated charge carriers, enabling effective breakdown of dye molecules under light irradiation. This makes ZnS nanostructures an ideal material for environmental remediation tasks, including water purification and pollutant degradation.

Table 1 The estimated structural parameters of as-grown transparent nanostructured ZnS ultrathin film

Peak Position $2\theta°$	FWHM (β)	Planes (hkl)	Crystallite size (D) nm	Dislocation Density $\partial = 1/D^2$ nm^{-2}	Microstrain ϵ
28.38	0.59	(111)	13.87	0.005	0.002
34.27	0.29	(200)	28.15	0.001	0.001
47.11	0.59	(220)	14.67	0.004	0.002
56.51	0.29	(311)	30.53	0.001	0.001
59.62	0.78	(222)	11.62	0.007	0.003
63.17	0.59	(400)	15.78	0.004	0.002
Average values			19.11	0.004	0.002

3.2.2 FESEM Analysis

Field Emission Scanning Electron Microscopy (FESEM) is a powerful imaging technique that provides detailed, high-resolution images of sample surfaces by scanning them with a focused electron beam. It allows for the examination of microstructures and morphology at magnifications up to several hundred thousand times, making it invaluable in materials science. FESEM analysis of the ZnS thin film as shown in Fig. 3 reveals a surface densely populated with nanorods. The image, taken at a magnification of 10,000×, shows that the nanorods are elongated and rectangular in shape, with a length of 250 nm and a width of 78 nm. The nanorods are well-dispersed across the substrate, although some clustering is observed due to the strong agglomeration of smaller nanorods. The micrograph highlights the uniformity in size and shape of the nanorods, suggesting a controlled synthesis process. The high-resolution imaging, conducted with an Everhart-Thornley Detector at an accelerating voltage of 15.00 kV and a working distance of 9.6 mm, provides a clear view of the nanostructures, indicating a successful deposition of ZnS nanorods. Inset of Fig. 3 represents the histogram of particle size distribution of ZnS nanorods obtained from SEM analysis, fitted with a Gaussian curve to highlight the mean particle size and size variation [25].

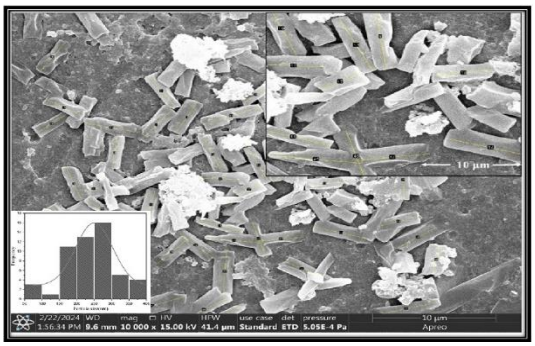

Fig. 3 FESEM analysis of as deposited ZnS thin film with an inset shown histogram of particle size distribution of ZnS nanorods with Gaussian fit (Mean = 250nm)

The significance of these findings lies in the implications for the photocatalytic properties of the ZnS nanorods. The uniform nanorod morphology and nanoscale dimensions enhance the surface area available for photocatalytic reactions, thereby improving the adsorption of reactants such as methyl red dye and maximizing the interaction with light. The elongated structure promotes effective charge carrier

https://doi.org/10.30799/jnst.359.25100301

Cite this Article as: Deepti Gupta, Trapti Gupta, Ramphal Sharma, Gunjan Soni, Solution-grown transparent ZnS ultra-thin nanostructured films for photocatalytic degradation of methyl red, J. Nanosci. Tech. 10(3) (2025) 1006–1011.

separation, reducing electron-hole recombination, which is critical for achieving high photocatalytic efficiency. Additionally, the high crystallinity and well-defined morphology reduce scattering losses and improve photon absorption, further boosting the material's photocatalytic activity. The well-dispersed nanorods, despite slight agglomeration, ensure adequate exposure of active sites to the surrounding environment, facilitating effective dye degradation. These structural and morphological features make the ZnS thin film highly promising for applications in photocatalytic water purification, particularly in the degradation of methyl red dye, where uniformity, high surface area, and efficient charge separation are crucial for optimal performance. The findings underline the potential of ZnS nanorods as an efficient photocatalyst for addressing environmental pollution.

3.2.3 EDAX Analysis

As shown in Fig. 4, Energy dispersive X-ray analysis (EDAX) was performed to determine the elemental composition of the synthesized ZnS nanorods. The EDAX spectrum revealed distinct peaks for zinc (Zn) and sulfur (S), confirming their presence in the sample.

Quantitative analysis from the EDAX data indicated an elemental composition of 41.1 wt% zinc (Zn) and 58.9 wt% sulfur (S), corresponding to an atomic ratio of approximately 1:1 [26]. This 1:1 stoichiometric ratio is ideal for photocatalytic activity as it ensures the absence of excess sulfur or zinc, which could introduce unwanted defects or secondary phases, such as zinc oxide (ZnO) or sulfur clusters. These impurities could act as recombination centers for photogenerated electron-hole pairs, significantly reducing the photocatalytic efficiency. Achieving accurate stoichiometry is therefore critical for maintaining the material's high crystalline quality, optimizing charge carrier dynamics, and ensuring efficient light absorption and surface reactivity.

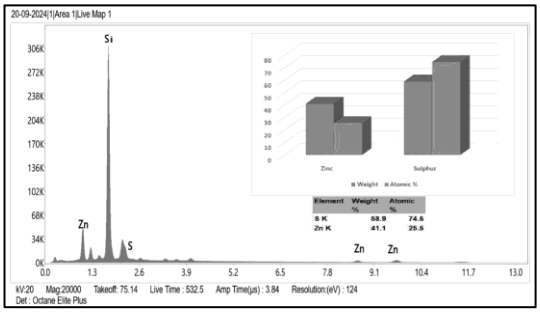

Fig. 4 EDAX spectrum analysis of nanostructured ZnS ultra thin film annealed at 100 °C in an air atmosphere and inset shows the relative atomic % and weight percentage for Zn and S elements

The high-purity stoichiometric ZnS obtained in this study is crucial for achieving the desired optical and electronic properties necessary for efficient photocatalytic performance. The EDAX analysis complements the XRD findings, collectively verifying the successful synthesis of high-purity ZnS nanorods with the appropriate elemental composition for advanced photocatalytic applications, such as dye degradation in water purification systems.

3.2.4 FTIR Spectrum Analysis

The FTIR spectrum of nanostructured ZnS, as shown in Fig. 5, reveals significant improvements in vibrational modes, indicating enhanced structural and compositional quality. The Zn-S vibrational modes observed in the range of 600–700 cm^{-1} exhibit increased sharpness and intensity, reflecting improved crystallinity and a denser ZnS structure. Peaks associated with impurities in the 1000–1500 cm^{-1} range show reduced intensity, suggesting the partial removal of residual organic compounds, likely originating from the alcohol used during the cleaning of the FTIR crucible. Additionally, a prominent peak at 3351 cm^{-1} corresponds to O-H stretching vibrations, which may be due to trace amounts of adsorbed water on the film surface [19, 20, 23]. Further, impurity-related peaks in the 1500–1700 cm^{-1} range are narrower and less intense, indicating a decrease in contamination levels.

The improved crystallinity, reduced impurities, and lower moisture content are crucial for optimizing the photocatalytic performance of the ZnS nanorods. Better crystallinity ensures efficient charge carrier dynamics, reduced impurities minimize recombination centers for electron-hole pairs, and lower moisture content prevents unwanted side reactions, all of which contribute to enhanced photocatalytic activity, particularly in applications like dye degradation. These findings collectively emphasize the superior structural integrity and reduced impurities in the nanostructured ZnS thin films.

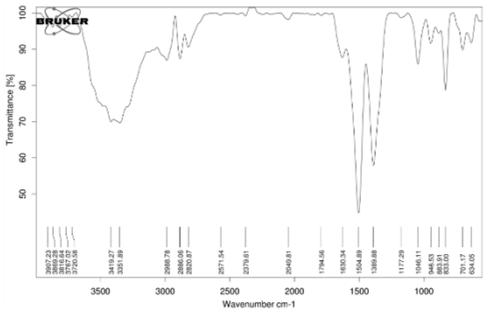

Fig. 5 FTIR spectrum of transparent nanostructured zinc sulfide (ZnS) ultra thin film

3.2.5 Film Thickness

The thickness of the ZnS thin films was measured using the gravimetric method with a highly sensitive microbalance. The calculation was performed using the formula,

$$t = M / \rho A \quad (5)$$

where M is the mass of the deposited film, ρ is the density of ZnS, and A is the area of the film. As shown in Table 2, the thickness of ZnS thin films deposited for 1, 2, 3, and 4 hours was found to be 0.3185 nm, 1.8578 nm, 2.1356 nm, and 2.3042 nm respectively.

3.2.6 UV-Visible Spectroscopy

UV-Visible Spectroscopy has been carried out to determine the optical transparency and bandgap of deposited ZnS thin films as shown in Fig. 6(i) and (ii). The optical absorption of the ZnS thin film was studied with the help of UV–Vis spectrophotometer in the wavelength range of 300–800 nm. Fig. 7(i) illustrates the UV-Vis absorption spectra of ZnS thin films deposited for varying durations (1 hour, 2 hours, 3 hours, and 4 hours). In Fig. 6(i) the absorbance graph reveals that absorbance increases with longer deposition times. The 1-hour deposition shows the lowest absorbance, while the 4-hour deposition exhibits the highest.

In Fig. 6(i) the absorption edge is observed to shift with increasing deposition time, indicating a potential change in film thickness and crystallinity. Notably, the thin film deposited for 4 hours exhibits distinct absorption shoulders at 442 nm and 563 nm, signifying enhanced absorption in the visible region. This behaviour is attributed to improved film quality and the formation of shallow defect states, which facilitate electronic transitions.

The visible light absorption by the 4-hour ZnS thin film highlights its suitability for photocatalytic applications under sunlight. In contrast, films deposited for shorter durations (1 - 3 hours) show relatively lower absorbance across the entire visible range, suggesting insufficient film thickness and a lower density of active sites. These results demonstrate that the deposition time significantly influences the optical properties of ZnS thin films, with the 4-hour film being the most promising candidate for sunlight-driven photocatalytic degradation of methyl red.

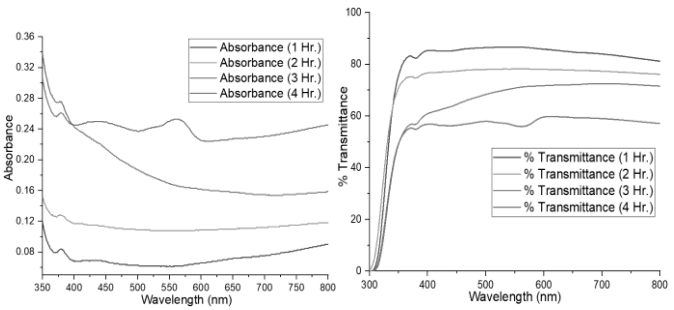

Fig. 6 Variation of (i) absorbance and (ii) transmittance with wavelength at varying deposition time

Fig. 6(ii) depicts the transmittance spectra of ZnS thin film grown on the glass substrate. The films exhibited highly transparent in the visible region. For instance, the transmission for the film deposited at 1 hour was over 80%, and the film deposited at 2 hours exhibited 78% transmittance in the visible region. All the prepared films had a sharp absorption edge. The sharp absorption edge and high transmission percentage represent a high quality of the prepared films, such as lack of pinhole and crack as well as the formation of the uniform particles in size and shape. It can also be noticed that as the deposition time increases, the percentage transmittance of the material decreases. Specifically, the highest transmittance is observed for the 1-hour deposition, while the lowest transmittance is noted for the 4-hour deposition. Initially, all samples

https://doi.org/10.30799/jnst.359.25100301

show a sharp increase in transmittance from 300 nm to about 400 nm, followed by a plateau up to 800 nm. This suggests that shorter deposition times result in a more transparent material.

The inverse relationship between transmittance and absorbance as deposition time increases can be attributed to several factors. Longer deposition times result in thicker films, which absorb more light and thus transmit less. Additionally, extended deposition might introduce more defects and impurities, increasing light absorption and scattering, and thereby reducing transmittance. Changes in the film's density and chemical composition with prolonged deposition can further enhance absorbance. Surface roughness, which may increase with deposition time, can scatter light more effectively, reducing direct transmittance and increasing absorbance. Moreover, variations in grain size or crystallinity associated with longer deposition times can affect the material's optical properties, leading to higher absorbance. As shown in Fig. 7, the band gap energy of the film was calculated from the Tauc plot based on the equation below,

$$(\alpha h\upsilon)^{1/n} = A(h\upsilon - E_g) \quad (6)$$

where hυ denotes the incident photons energy, α resembles the absorption coefficient, A is a material constant, and n = 1/2 is for direct band gap ZnS semiconductor. The band gap energy (E_g) is obtained from the extrapolation of the linear portions with respect to the plots onto the x-axis. Other than that, plots of $(\alpha h\upsilon)^2$ versus (hυ) are made for ZnS NP's. As shown in Fig. 8, the band gap energy for 1, 2, 3, and 4 hour deposited thin film of ZnS was 3.79 eV, 3.75 eV, 3.70 eV, and 3.66 eV respectively. A decreasing trend in bandgap energy is observed with increasing deposition time, as summarized in Table 2.

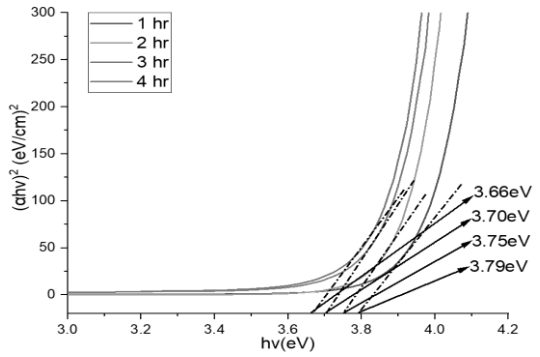

Fig. 7 Band gap shift at different deposition time intervals in nanostructured ZnS ultra thin films before dye degradation

Table 2 Band gap, blue shift and thickness of as-grown transparent nanostructured ZnS ultrathin film at different deposition time

Deposition time (hour)	Band gap(eV)	Blue shift w.r.t. bulk (ΔE) eV	Thickness (nm)
1	3.79	0.25	0.3185
2	3.75	0.21	1.8578
3	3.70	0.16	2.1356
4	3.66	0.12	2.3042

The bandgap reduction with prolonged deposition time is primarily due to the increase in film thickness [6]. Thicker films enhance the localized density of states near the band edges, narrowing the bandgap. Additionally, the decrease in strain and the absence of charge accumulation at grain boundaries contribute to the bandgap narrowing. The results confirm that increasing deposition time improves film thickness [27] and optical absorption while decreasing the bandgap, making the films more suitable for applications such as photocatalytic degradation of methyl red under sunlight [6,16,23].

3.2.7 Photocatalytic Degradation of Methyl Red Dye and Its Application in Water Purification

The Tauc plots shown in Fig. 8 illustrates the optical bandgap energy (Eg) variations during the photocatalytic degradation of methyl red dye under sunlight at different time intervals (10, 30, 40, 50, and 60 minutes). The X-axis represents the photon energy (hv) in electron volts (eV), while the Y-axis corresponds to $(\alpha hv)^2$, which is proportional to the optical absorption. As the degradation time increases, the intercept of the linear regions of the curves with the x-axis shifts slightly to the right, indicating increase in the material's bandgap energy. These bandgap values, calculated from the extrapolated linear portions, ranges from 3.97 eV to 4.24 eV. The observed increase in bandgap energy with time suggests modifications in the electronic structure of the photocatalyst, possibly due to changes in its surface or chemical composition during the degradation process. This shift may result from the removal of adsorbed dye molecules or the formation of reaction intermediates, revealing the intrinsic properties of the photocatalyst. The changes in the absorption edge reflect the photocatalyst's efficiency in degrading methyl red dye under sunlight. Overall, the Tauc plot provides valuable insights into the dynamic optical properties and photocatalytic mechanism during the degradation process.

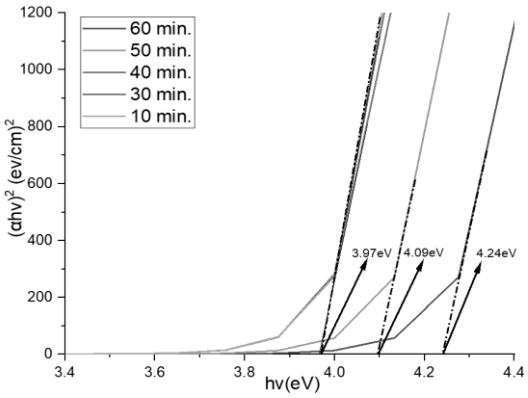

Fig. 8 Band gap shift at different time intervals in nanostructured ZnS ultra thin films after dye degradation

3.3 Mechanism of Action

Fig. 9 illustrate the proposed mechanism responsible for the enhanced photocatalytic activity observed in ZnS nanoparticles [25].

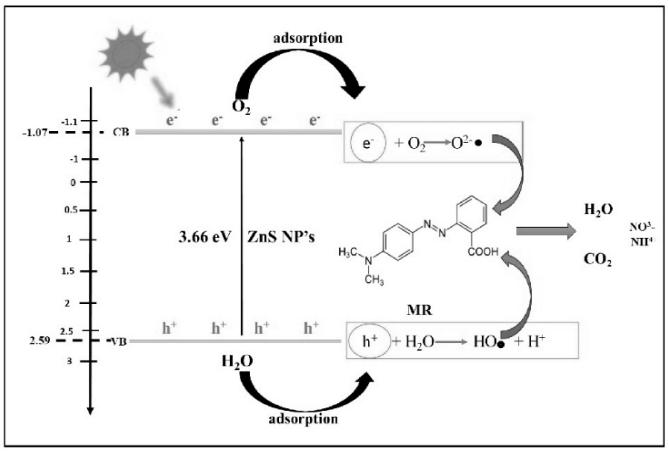

Fig. 9 Schematic representation of photocatalytic degradation mechanism of methyl red dye using ZnS NP's under visible light irradiation for 1 Hr

3.3.1 Photoexcitation of ZnS

Zinc sulfide (ZnS) absorbs light energy (hv) greater than or equal to its bandgap, producing charge carriers a photogenerated electron (e^-) in the conduction band (CB) with sufficient reduction power, and photogenerated holes (h^+) in the valence band (VB) with high oxidation power, are essential for efficient photocatalytic reactions.

$$ZnS + h\nu \rightarrow e- + h^+$$

3.3.2 Formation of Reactive Oxygen Species (ROS)

i. Superoxide Anion ($O^{\cdot}{}_2^-$)

The photogenerated electron (e^-) reduces adsorbed molecular oxygen (O_2) to form a superoxide anion radical.

$$e^- + O_2 \rightarrow O^{\cdot}{}_2^-$$

ii. Hydroxyl Radicals ($^{\cdot}OH$)

The photogenerated hole (h^+) oxidize water (H_2O) or hydroxide ions (OH−) absorbed on the catalyst's surface, to form hydroxyl free radical.

$$h^+ + H_2O \rightarrow {}^{\cdot}OH + H+$$

$$h^+ + OH- \rightarrow {}^{\cdot}OH$$

However, identifying the major contributor between ROS species is very critical. The generation of ROS and their environment in the oxidation of methyl red primarily relies on the appropriate potential of the band

https://doi.org/10.30799/jnst.359.25100301

edges inherent in a photocatalyst. Hence, the following equations have been employed to compute the conduction band potential (E_{CB}) and valence band potential (E_{VB}) of ZnS [3]:

$$E_{CB} = X - E_e - E_g/2$$

$$E_{VB} = E_{CB} + E_g$$

Here, X represents the geometric mean of the absolute electronegativity of the constituent atoms, Ee is the energy of free electrons on the hydrogen scale (~4.5 eV), and Eg is the bandgap energy of the photocatalyst. For ZnS, the Pearson absolute electronegativity values for Zn and S are 4.34 eV and 6.18 eV, respectively, yielding a calculated bandgap energy (Eg) of 3.66 eV based on a Tauc plot. Substituting these values, the E_{CB} and E_{VB} for ZnS were calculated to be -1.07 eV and +2.59 eV, respectively [28].

The negative value of ECB (-1.07 eV) indicates that ZnS has a conduction band potential that is more negative than the reduction potential of O_2 to O_2^- (-0.28 eV). This confirms that electrons in the conduction band of ZnS can effectively generate superoxide anion radicals (O_2^-). Similarly, the positive EVB value (+2.59 eV) indicates that holes in the valence band of ZnS have sufficient potential to generate hydroxyl radicals (•OH) by oxidizing water or hydroxide ions. These calculated band positions highlight the crucial role of bandgap energy in photocatalytic reactions, as it directly influences the generation of reactive oxygen species (ROS). The ability of ZnS to produce both superoxide anions and hydroxyl radicals demonstrates its efficacy as a photocatalyst for the degradation of organic pollutants like methyl red.

3.3.3 Oxidative Degradation of Methyl Red

ROS attack methyl red molecules, leading to their breakdown into smaller, non-toxic intermediates and final degradation products. The primary contributors are hydroxyl radicals and superoxide ions [25].

$$^{\cdot}OH\ /O^{\cdot}{}_2^- + \text{Methyl Red} \rightarrow \text{Degradation Products}$$

4. Conclusion

ZnS nanostructured thin films were synthesized using the CBD method and comprehensively characterized. SEM and XRD analysis confirmed the formation of nanorod-like structures and improved crystallinity, while FTIR results indicated reduced impurities and enhanced structural integrity. UV-Vis spectral analysis revealed a significant blue shift (3.66 eV), correlating with efficient photocatalytic activity in methyl red dye degradation. A degradation efficiency of 97% was achieved within 60 minutes. These findings establish ZnS thin films as an effective, sustainable, and cost-efficient photocatalyst for water purification and future environmental technologies.

Acknowledgments

The authors would like to express their deepest gratitude to the Chancellor of IIS (Deemed to be) University, Dr. Ashok Gupta, for his invaluable support and encouragement throughout the course of this research. Their guidance and belief in the importance of this work have been instrumental in its completion. Authors are profoundly grateful for the resources and opportunities provided under their leadership, which have significantly contributed to the success of this project. Additionally, one of the authors, Prof. Ramphal Sharma, extends his thanks to the CURIE project (Ref. No. DST/CURIE-02/2023/IISU) funded by GOI DST New Delhi for the financial support.

Author Contributions

The authors contributed to this research as follows: Deepti Gupta conducted the experimental work, ensuring precise execution and reliable data collection. Trapti Gupta was responsible for the conceptualization of the study and the development of the methodology, aligning the research design with the objectives. Ramphal Sharma provided critical review and visualization of the results, enhancing the overall quality and presentation of the work. Gunjan Soni assisted in the research process by supporting data collection and analysis.

Conflicts of Interest: The authors declare no conflict of interest.

References

[1] H. Kaur, S. Kumar, P. Kumar, A.A. Ghfar, G. Bouzid, Tailoring ZnS nanostructures through precipitation-cum-hydrothermal synthesis for enhanced wastewater purification and antibacterial treatment, Environ. Res. 259 (2024) 119534.
[2] K. Sharma, P. Raizada, V. Hasija, P. Singh, A. Bajpai, V.H. Nguyen, et al., ZnS-based quantum dots as photocatalysts for water purification. J. Water Proc. Eng. 43 (2021) 102217.
[3] L. Isac, A.Enesca, Recent developments in ZnS-based nanostructures photocatalysts for wastewater treatment, Int. J. Mol. Sci. 23(24) (2022) 15668.
[4] M. Sharma, T. Jain, S. Singh, O.P. Pandey, Photocatalytic degradation of organic dyes under UV-Visible light using capped ZnS nanoparticles. Solar Ener. 86(1) (2012) 626-633.
[5] T. Ben Nasr, N. Kamoun, M. Kanzari, R. Bennaceur, Effect of pH on the properties of ZnS thin films grown by chemical bath deposition, Thin Solid Films 500 (2006) 4-8.
[6] A. Kumar, S. Mukherjee, S. Sahare, R.K. Choubey, Influence of deposition time on the properties of ZnS/p-Si heterostructures, Mater. Sci. Semicond. Process. 122 (2021) 105471.
[7] N. Dengo, A. Vittadini, M.M. Natile, S. Gross, In-depth study of ZnS nanoparticle surface properties with a combined experimental and theoretical approach, J. Phys. Chem. C 124(14) (2020) 7777-7789.
[8] Z. Ye, L. Kong, F. Chen, Z. Chen, Y. Lin, C. Liu, A comparative study of photocatalytic activity of ZnS photocatalyst for degradation of various dyes, Optik (Stuttg) 164 (2018) 345-354.
[9] N. Tripathy, R. Ahmad, H. Kuk, D.H. Lee, Y.B. Hahn, G. Khang, Rapid methyl orange degradation using porous ZnO spheres photocatalyst, J. Photochem. Photobiol. B. 161 (2016) 312-317.
[10] J.A. Khan, S. Ahamad, M.A.H. Ansari, M. Tauqeer, C-H. Park, J.P. Park, et al., State-of-the-art in ZnS-based nanoarchitects for visible-light photocatalytic degradation of antibiotics and organic dyes, J. Water Process Eng. 67 (2024) 106151.
[11] P. Ahuja, S.K. Ujjain, R. Kanojia, P. Attri, Transition metal oxides and their composites for photocatalytic dye degradation, J. Compos. Sci. 5 (2021) 5030082.
[12] R.S. Mane, C.D. Lokhande, Chemical deposition method for metal chalcogenide thin films, Mater. Chem. Phys. 65 (2000) 1-31.
[13] H. Abdullah, N.H. Saadah, S. Shaari, A. Muchtar, Optical and structural properties of ZnS thin films grown by CBD technique, Adv. Mater. Res. 139-141 (2010) 149-152.
[14] R. Zein, I. Alghoraibi, Influence of bath temperature and deposition time on topographical and optical properties of nanoparticles ZnS thin films synthesized by a chemical bath deposition method, J. Nanomater. 2019 (2019) 541863.
[15] Z.Q. Li, J.H. Shi, Q.Q. Liu, Z.A. Wang, Z. Sun, S.M. Huang, Effect of [Zn]/[S] ratios on the properties of chemical bath deposited zinc sulfide thin films, Appl. Surf. Sci. 257 (2010) 122-126.
[16] G. Arandhara, J. Bora, P.K. Saikia, Effect of pH on the crystallite size, elastic properties and morphology of nanostructured ZnS thin films prepared by chemical bath deposition technique, Mater. Chem. Phys. 241 (2020) 122277.
[17] A. Chakrabarti, E. Alessandri, Syntheses, properties, and applications of ZnS-based nanomaterials, Appl. Nano. 5(3) (2024) 116-142.
[18] S.K. Maji, A.K. Dutta, D.N. Srivastava, P. Paul, A. Mondal, B. Adhikary, Effective photocatalytic degradation of organic pollutant by ZnS nanocrystals synthesized via thermal decomposition of single-source precursor, Polyhedron 30(15) (2011) 2493-2498.
[19] O.M. Hameed, Synthesis of zinc sulfide nanocrystals by chemical bath deposition methods, In: E3S Web of Conferences, ICMED-ICMPC 391 (2023) 01134.
[20] M. Jothibas, S. Johnson Jeyakumar, C. Manoharan, I. Kartharinal Punithavathy, P. Praveen, J. Prince Richard, Structural and optical properties of zinc sulphide nanoparticles synthesized via solid state reaction method, J. Mater. Sci.: Mater. Electronic. 28 (2017) 1889-1894.
[21] S. Tec-Yam, J. Rojas, V. Rejón, A.I. Oliva, High quality antireflective ZnS thin films prepared by chemical bath deposition, Mater. Chem. Phys. 136 (2012) 386-393.
[22] A. Goudarzi, S.M. Langroodi, M. Arefkhani, N. Samadani Langeroodi, Study of optical properties of ZnS and MnZnS (ZnS/MnS) nanostructure thin films; Prepared by microwave-assisted chemical bath deposition method, Mater. Chem. Phys. 275 (2022) 125103.
[23] N. Chabou, B. Birouk, M.S. Aida, J.P. Raskin, Deposition time and annealing effects on morphological and optical properties of ZnS thin films prepared by chemical bath deposition, Mater. Science- Poland 38 (2020) 508-517.
[24] N. Bouguila, D. Bchiri, M. Kraini, A. Timoumi, I. Halidou, K. Khirouni, et al., Structural, morphological and optical properties of annealed ZnS thin films deposited by spray technique, J. Mater. Sci.: Mater. Electron. 26 (2015) 9845-9852.
[25] L. Lianmawii, N.M. Singh, Luminescence and photocatalytic degradation of indigo carmine in the presence of Sm^{3+}doped ZnS nanoparticles, Sci. Rep. 13 (2023) 22450.
[26] S. Biswas, S. Kar, S. Chaudhuri, Synthesis and characterization of zinc sulfide nanostructures, Synthesis and Reactivity in Inorganic, Metal-Organic and Nano-Metal Chem. 36 (2006) 33-36.
[27] A.U. Ubale, D.K. Kulkarni, Preparation and study of thickness dependent electrical characteristics of zinc sulfide thin films, Bull. Mater. Sci. 28 (2005) 43-47.
[28] A.H. Ajil, N.M. Ahmed, F.K. Yam, Z.U. Zango, I.A. Wadi, M.A. Binzowaimil, et al., Enhancing methyl orange degradation with laser-generated ZnO and Ce-doped ZnO nanoparticles. App. Sci. 13 (2023) 11857.

https://doi.org/10.30799/jnst.359.25100301

Cite this Article as: Deepti Gupta, Trapti Gupta, Ramphal Sharma, Gunjan Soni, Solution-grown transparent ZnS ultra-thin nanostructured films for photocatalytic degradation of methyl red, J. Nanosci. Tech. 10(3) (2025) 1006–1011.